

Supporting Information

Adsorption of Hyperbranched Arabinogalactan-Proteins from Plant Exudate at Solid-Liquid Interface

Athénaïs Davantès ¹, Michaël Nigen ², Christian Sanchez ², Angelina d'Orlando ³ and Denis Renard ^{1,*}

¹ UR1268 Biopolymères Interactions Assemblages, INRA, F-44300 Nantes, France; athenais.davantes@inra.fr; denis.renard@inra.fr; angelina.d'orlando@inra.fr

² UMR IATE, UM-INRA-CIRAD-Montpellier Supagro, 2 Place Viala, F-34060 Montpellier Cedex, France; Nigen@supagro.inra.fr; christian.sanchez@supagro.inra.fr

* Correspondence: denis.renard@inra.fr; Tel.: +33 2 40 67 50 52

Table S1. Biochemical composition and structural parameters of *A. senegal* and *A. seyal* gums.

	<i>A. senegal</i> ¹	<i>A. seyal</i> ²
Moisture (%)	10.7	11.4
Sugar (%)		
Arabinose	29.8	47.6
Galactose	38.5	36.9
Rhamnose	12.8	3.0
Glucuronic acid	17.9	6.7
4-O-Me-Glucuronic acid	1.0	5.8
Uronic acid / neutral sugar ratio	0.23	0.14
Protein (%) ^a	2.0 (27) ^b	1.0 (29) ^b
Mineral (%)	3.4	4.0
Average molecular weight (M _w , g.mol ⁻¹)	6.5 x 10 ⁵	8.2 x 10 ⁵
Polydispersity index (M _w /M _n)	2.2	1.5
High M _w AGP (%)	15.4	20
Branching degree (%)	78.0	59.2
Intrinsic viscosity (mL.g ⁻¹) ^c	30.2	16.5
Number of negative charges	560	452
R _g (nm)	28.6	17.1
R _h (nm)		
Dynamic light scattering	15 ^d , 16 ^e	13 ^d , 14 ^e
Viscosimetry	15	14

¹from Apolinar-Valiente et al. (2018) Food Hydrocolloids 89 pp. 864-873 (47); ²from Lopez Torrez et al. (2015) Food Hydrocolloids 51 pp. 41-53 (6); ^a Protein content was measured using the Kjeldhal method; ^b Percentage of nonpolar aminoacids; ^c Measured using differential capillary viscometry (on line size exclusion chromatography system) in 100 mM LiNO₃ (pH 5.0) solution containing 0.02% NaNO₃; ^d Hydrodynamic radius (R_h) in sodium acetate 10 mM pH 5; ^e Hydrodynamic radius (R_h) in 100 mM LiNO₃ (pH 5.0)

Table S2. Electrophoretic mobility of *A. senegal* and *A. seyal* gums in solution (μ_e), films characteristics calculated from QCM-D and SPR data, and % water content (Γ_{H2O}) of *A. senegal* and *A. seyal* gum films after adsorption on gold substrate as a function of pH for a salt concentration of 10 mM.

	<i>A. senegal</i>			<i>A. seyal</i>		
pH	3.00 ± 0.05	5.00 ± 0.05	7.00 ± 0.05	3.00 ± 0.05	5.00 ± 0.05	7.00 ± 0.05
μ_e ($\mu\text{m.cm/V.s}$)	-1.31 ± 0.05	-1.74 ± 0.06	-2.06 ± 0.08	-1.08 ± 0.11	-1.40 ± 0.12	-1.64 ± 0.08
Rearrangements (D-f plot)	2	1	1	1	1	2
Shear viscosity η ($\mu\text{Pa.s}$)	1007 ± 57	1287 ± 14	844 ± 18	2143 ± 60	1508 ± 213	954 ± 145
Shear elastic modulus μ_f (kPa)	125 ± 0.6	94 ± 1	61 ± 1	217 ± 6	131 ± 83	77 ± 15
$\Gamma_{\text{QCM-D}}$ (ng/cm ²)	407 ± 180	1162 ± 16	1675 ± 64	240 ± 23	231 ± 24	274 ± 31
d _{QCM-D} (nm)	2.4 ± 0.1	6.8 ± 0.1	9.8 ± 0.4	1.4 ± 0.1	1.3 ± 0.1	1.6 ± 0.2
Desorption QCM-D	11.0 %	3.3 %	0.3 %	15.8 %	15.8 %	7.0 %
Γ_{SPR} (ng/cm ²)	155 ± 9	105 ± 6	242 ± 15	92 ± 6	40 ± 2	124 ± 8
d _{SPR} (nm)	0.9 ± 0.05	0.6 ± 0.04	1.4 ± 0.08	0.5 ± 0.03	0.2 ± 0.01	0.7 ± 0.04
Desorption SPR (%)	3.8	1.0	0.1	1.2	11.0	0.9
$\Gamma_{\text{H}_2\text{O}}(\%)$	61.9	91.0	85.5	61.7	82.5	54.7

Table S3. Electrophoretic mobility of *A. senegal* and *A. seyal* gums in solution (μ_e), films characteristics calculated from QCM-D and SPR data, and % water content ($\Gamma_{\text{H}_2\text{O}}$) of *A. senegal* and *A. seyal* gum films after adsorption on gold substrate as a function of salt concentration for a constant pH 5.0.

	<i>A. senegal</i>			<i>A. seyal</i>		
Salt concentration (mM)	1	10	100	1	10	100
μ_e ($\mu\text{m.cm/V.s}$)	-1.79 ± 0.06	-1.74 ± 0.06	-1.21 ± 0.06	-1.55 ± 0.07	-1.40 ± 0.12	-0.78 ± 0.14
Rearrangements (D-f plot)	1	1	1	2	1	1
Shear viscosity η (mPa.s)	1215 ± 35	1287 ± 14	1052 ± 18	- ¹	1508 ± 213	1137 ± 102
Shear elastic modulus μ_f (MPa)	108 ± 39	94 ± 1	105 ± 3	- ¹	131 ± 83	141 ± 11
$\Gamma_{\text{QCM-D}}$ (ng/cm ²)	193 ± 18	1162 ± 16	1907 ± 148	116 ± 16	231 ± 98	543 ± 240
d _{QCM-D} (nm)	1.1 ± 0.1	6.8 ± 0.1	11.2 ± 0.9	0.7 ± 0.1	1.3 ± 0.1	3.1 ± 0.05
Desorption QCM-D	9.3 %	3.3 %	0.8 %	7.3 %	15.8 %	8.5 %
Γ_{SPR} (ng/cm ²)	- ²	105 ± 6	383 ± 23	- ²	40 ± 2	267 ± 16
d _{SPR} (nm)	- ²	0.6 ± 0.04	2.3 ± 0.1	- ²	0.2 ± 0.01	1.5 ± 0.1
Desorption SPR (%)	- ²	1.0	7.5	- ²	11.0	3.1
$\Gamma_{\text{H}_2\text{O}}(\%)$	- ²	91.0	79.9	- ²	82.5	50.8

¹ Voigt fitting failed, data calculated using Sauerbrey equation; ² SPR failed: salt concentration and gum adsorption too low

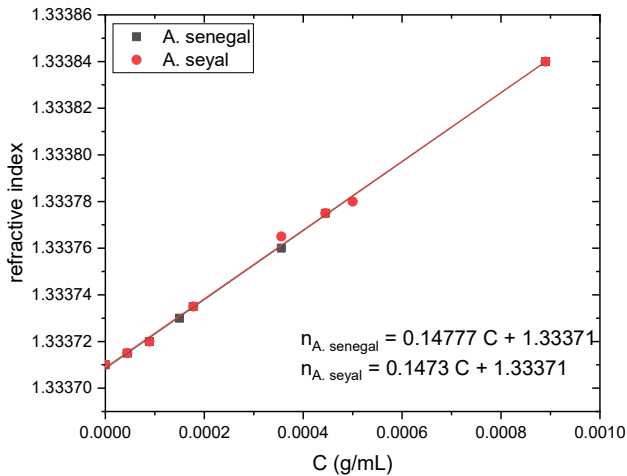


Figure S1. Refractive index ($\lambda = 589$ nm) of *A. senegal* and *A. seyal* in 10 mM acetate buffer pH 5.0 as a function of concentration. Linear fits give the slope corresponding to the refractive index increment dn/dC and extrapolation to $C = 1$ gives n_a , the refractive index of the adsorbed species in condensed form (i.e. corresponding to a “dry” film where 100% of gum species are adsorbed on gold surface).

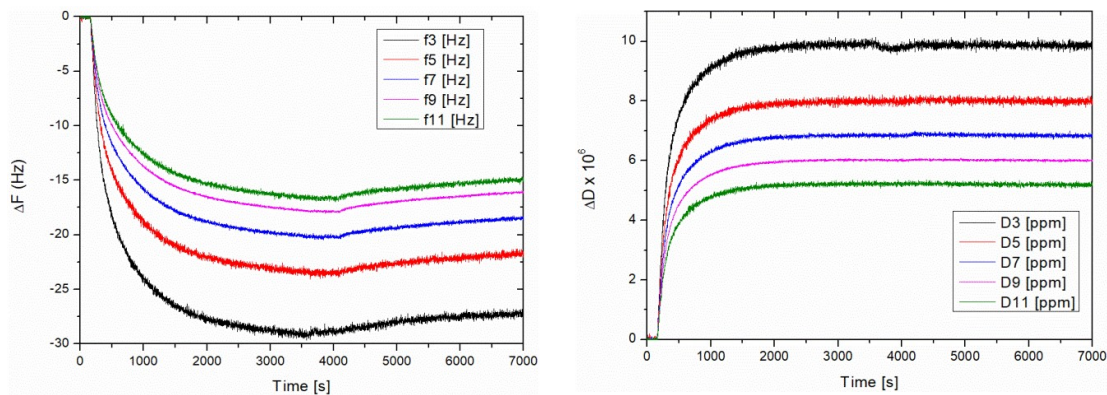


Figure S2. Adsorption of *A. senegal* gum at 150 ppm 10 mM acetate buffer pH 5.0 on gold substrate: frequency change (ΔF) and dissipation energy loss (ΔD) in time for five overtone frequencies

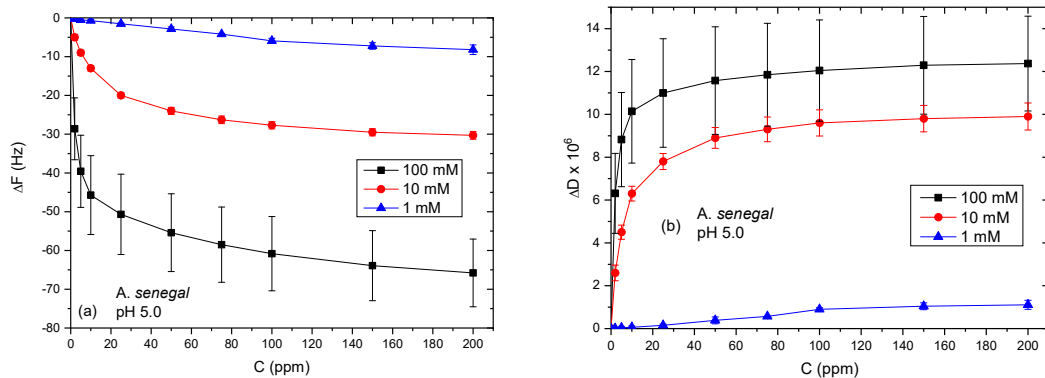


Figure S3. Adsorption isotherms of *A. senegal* gum on gold substrate presented as (a) frequency change (ΔF) and (b) dissipation energy loss (ΔD) at pH 5.0 and different salt concentrations (1, 10 and 100 mM).

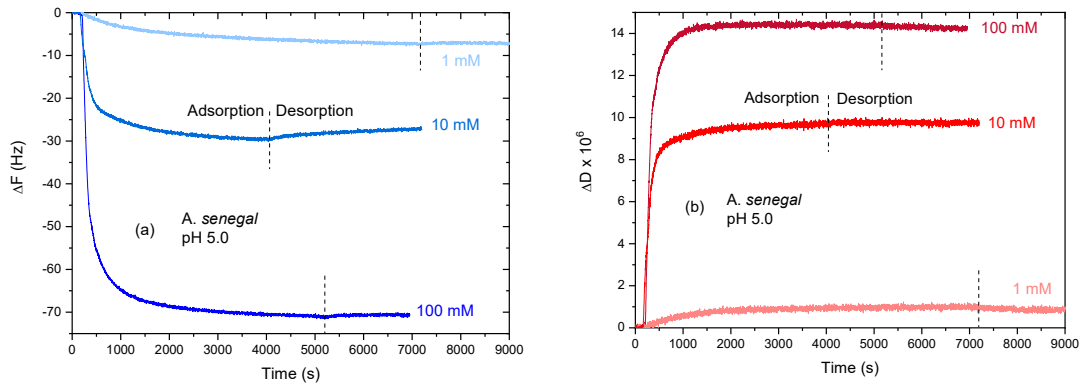


Figure S4. Adsorption kinetics of *A. senegal* gum at 150 ppm on gold substrate at pH 5.0: (a) frequency change (ΔF) and (b) dissipation energy loss (ΔD) for 1, 10 and 100 mM acetate buffer. Dashed lines represent the switch of solution from adsorption to desorption process with acetate buffer.

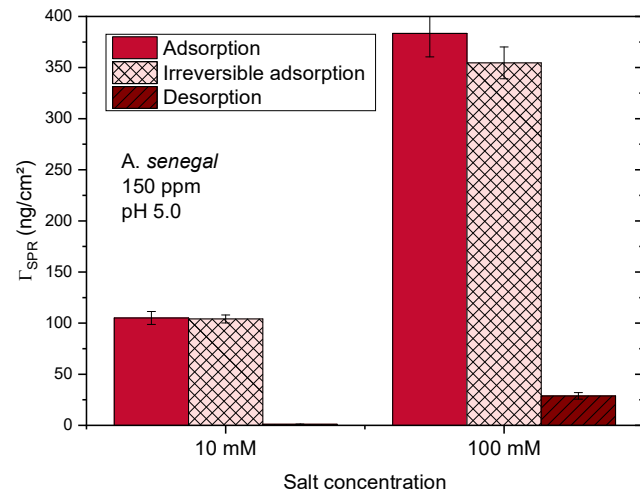


Figure S5 (revised). Comparison of the adsorbed amount Γ_{SPR} (ng.cm⁻²) at equilibrium on gold substrate of *A. senegal* gum at pH 5.0 as a function of salt concentration after adsorption and desorption (washed with buffer solution).

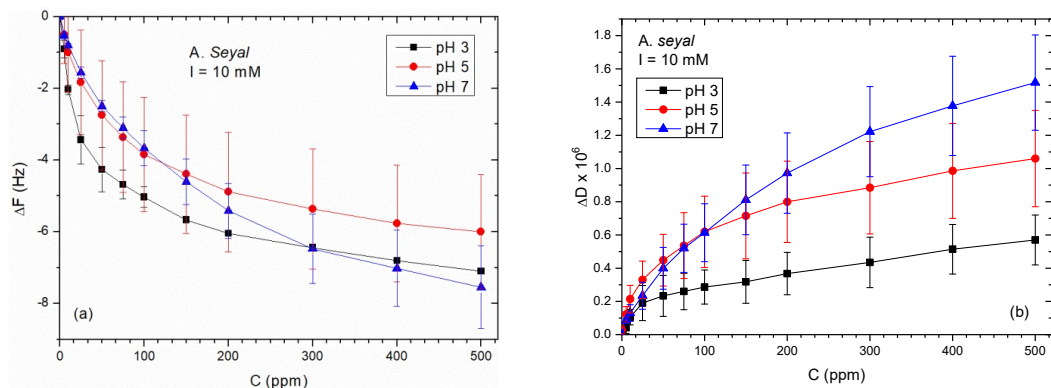


Figure S6. Adsorption isotherms of *A. seyal* gum on gold substrate presented as (a) frequency change (ΔF) and (b) dissipation energy loss (ΔD) as a function of pH (3.0, 5.0 and 7.0) and a constant salt concentration of 10 mM acetate buffer.

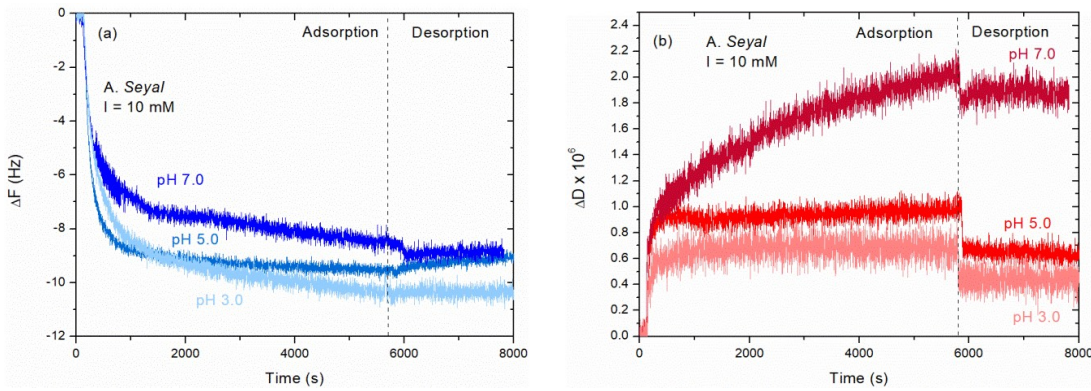


Figure S7. Adsorption kinetics of *A. seyal* gum at 500 ppm 10 mM acetate buffer on gold substrate as a function of pH: (a) frequency change (ΔF) and (b) dissipation energy loss (ΔD). Dashed lines represent the switch of solution from adsorption to desorption process with acetate buffer.

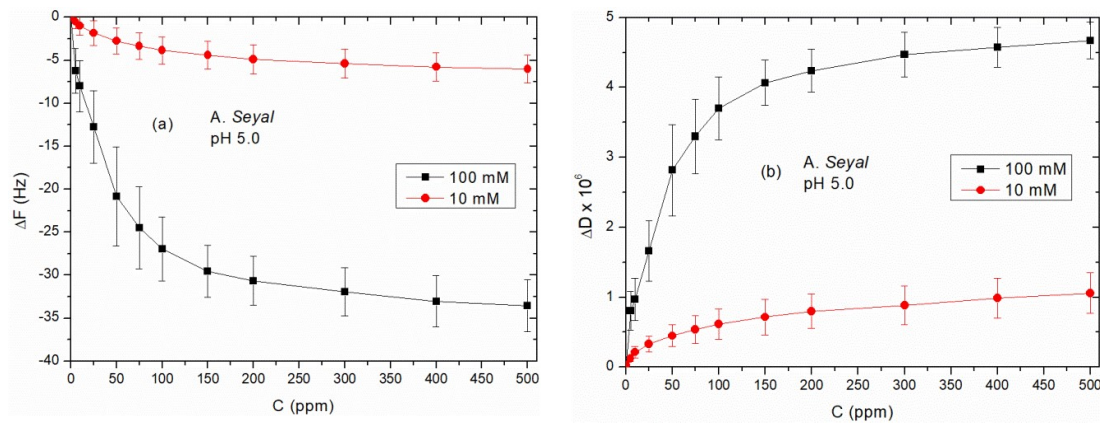


Figure S8. Adsorption isotherms of *A. seyal* gum on gold substrate presented as (a) frequency change (ΔF) and (b) dissipation energy loss (ΔD) with two salt concentrations: 10 and 100 mM at pH 5.0.

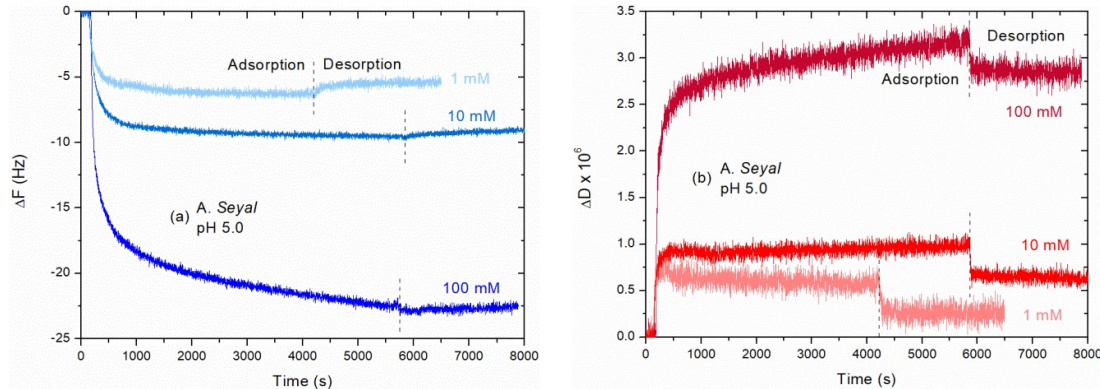


Figure S9. Adsorption of *A. seyal* gum at 500 ppm on gold at pH 5.0: (a) frequency change (ΔF) and (b) dissipation energy loss (ΔD) for 1, 10 and 100 mM acetate buffer. Dashed lines represent the switch of solution from adsorption to desorption process with acetate buffer.

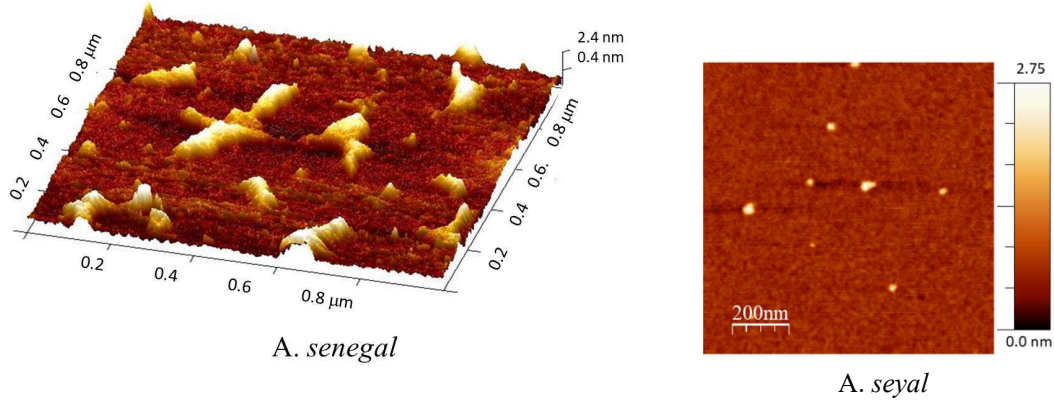


Figure S10. AFM topography images of *Acacia senegal* and *Acacia seyal* gums dry adsorbed layers on solid substrates at $1 \times 1 \mu\text{m}$.

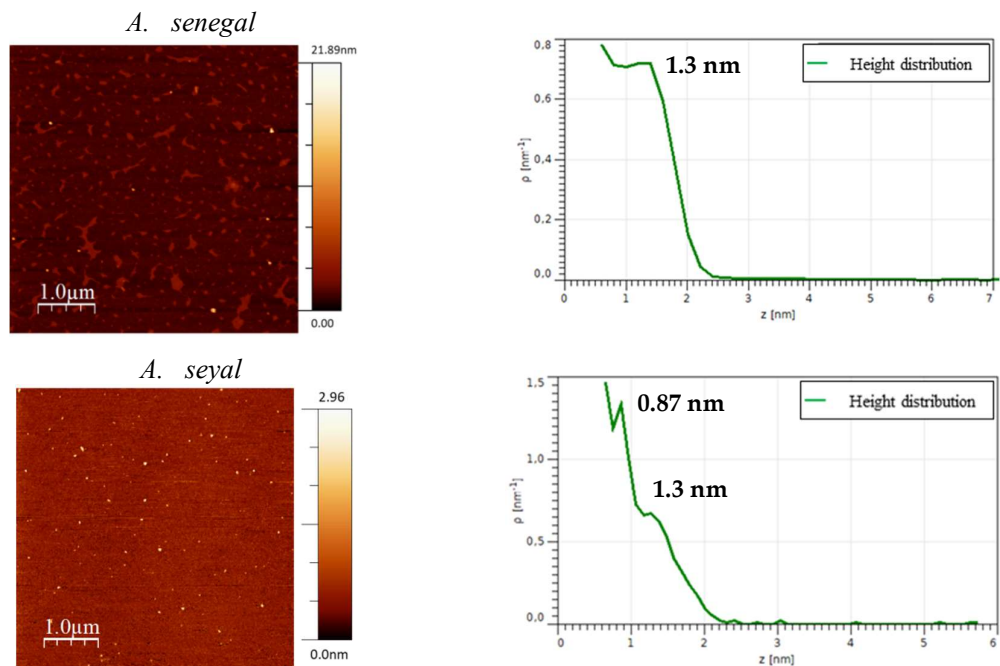


Figure S11. AFM topography images and height distributions of *Acacia senegal* and *Acacia seyal* gums dry adsorbed layers on solid substrates at $5 \times 5 \mu\text{m}$.

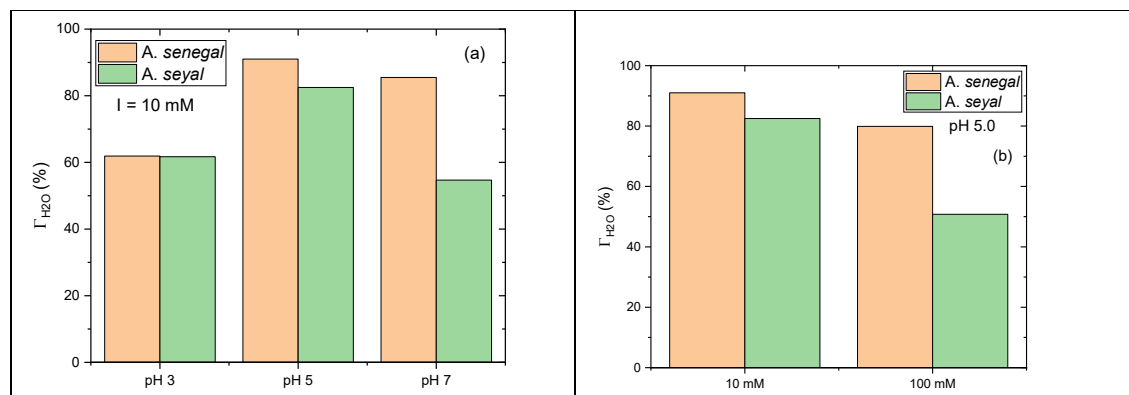


Figure S12. Hydration degree ($\Gamma_{\text{H}_2\text{O}}$, %) of *A. senegal* and *A. seyal* gum films as a function of pH (a) and salt concentration at pH 5.0 (b).

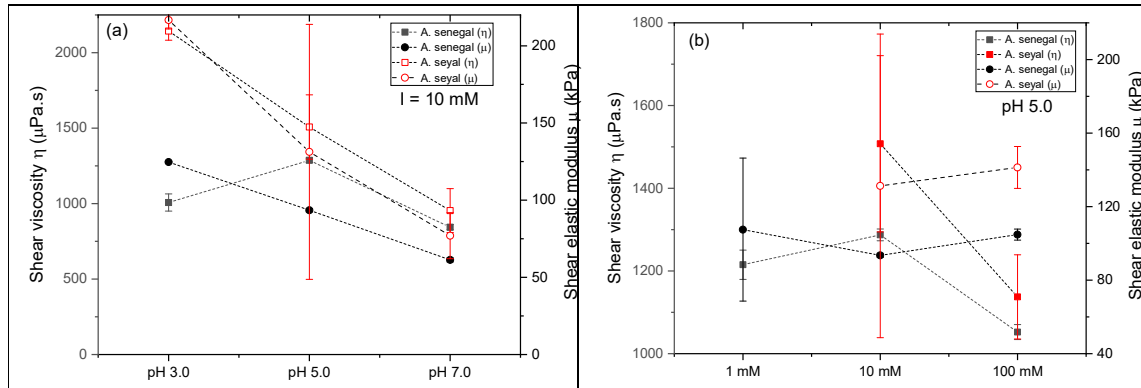


Figure S13. Viscoelastic properties derived from the Voigt model of *A. senegal* and *A. seyal* films as a function of pH (a) and salt concentration (b)